Separation and dissolution of Al_2O_3 inclusions at slag/metal interfaces

S.H. Lee, C. Tse, K.W. Yi*, P. Misra, V. Chevrier, C. Orrling, S. Sridhar and A.W. Cramb

Center of Iron and Steelmaking Research
Carnegie Mellon University
Pittsburgh, Pa 15213, USA
* School of Materials Sci. & Eng. Seoul National University
Seoul, 151-742 KOREA

Abstract

In order to achieve better process control and product quality in clean steel manufacturing, it is necessary to understand the underlying processes behind (i) separation of inclusions across slag/metal interfaces and (ii) dissolution of the inclusions in the slag. This paper presents novel results on both these processes obtained through *in situ* observations with a Confocal Scanning Laser Miscroscope at steelmaking temperatures.

In the case of separation, the considered system is the (Si,Mn)-killed steel/ CaO - Al_2O_3 slag (saturated with Al_2O_3) and it was found that liquid inclusion could be observed to separate across the interface into the slag side of the interface and dissolve rapidly. Solid Al_2O_3 inclusions were observed at the slag side of the interface and could be seen to agglomerate.

Dissolution of Al_2O_3 was studied in the following slag systems: SiO_2- Al_2O_3-CaO-MgO , SiO_2- Al_2O_3-CaO and Al_2O_3-CaO. The effects of temperature, slag viscosity and inclusion size will be elucidated.

Keywords: *Confocal-canning-laser microscopy, Clean steel, Inclusions, Separation, Slag/metal interface, Dissolution*

1. Introduction

The presence of non-metallic oxide inclusions is a major concern in many grades of commercial steel. Generally, inclusions degrade the mechanical properties of the steel by lowering the toughness of the cast metal and increasing the risk for mechanical and/or corrosive failure of the final product. Oxide inclusions are usually classified into two categories, (depending on their origin) [1]: (i) as residual products resulting from intentionally added alloying elements for de-oxidation in the ladle and (ii) as reaction products resulting from reactions between the melt and the atmosphere, slag or refractory. Examples of the latter, (often referred to as exogeneous or macro-inclusions) are results of re-oxidation of the molten metal and slag emulsification in the melt.

The specific requirements of allowable inclusion content and size varies according to application [1,2]; from < 5 μm diameter in ultra clean steel (for shadow masks in cathode ray tubes) to <100 μm diameter in sheet steel (for automotive sheets). However, a common constant is the need to minimize the amount and size of the inclusions and to control their distribution in the final product. Separating the inclusion from the molten metal into a slag phase, a priori to casting in the ladle, tundish or mold can minimize inclusion content. The process is schematically shown in Fig. 1 and involves [1]: (i) inclusion generation, (ii) transport of the inclusion to the interface, (iii) separation of the inclusion to the interface and (iv) removal of the inclusion from the interface.

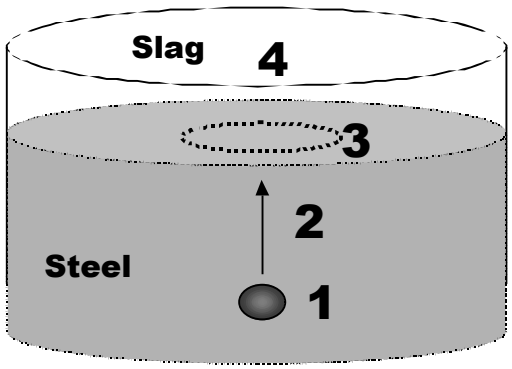

Figure 1. Inclusion generation and removal in an industrial vessel

While a lot of work has been conducted on the generation and bulk transport of inclusion little attention has been paid to the two final steps and it should be noted that inclusions are not removed from the melt until they have actually been incorporated into the slag. The final step involves the dissolution of the inclusion particle in the slag. Here, fast dissolution kinetics are desired since:

- the inclusions may rest near the interface and cause steric hindrance to further separation,
- as long as the inclusion remains at the interface there is risk for inclusion re-entrainment into the melt,
- in the case of mould slags, while dissolved inclusions of e.g. Al_2O_3 may decrease the crystallization index and thus prevent sticker breakouts, un-

dissolved inclusions act as inoculants and cause early crystallization [3] that may increase the risk of sticker breakouts [4] and

- a large amount of solid inclusions may change the viscosity in an undesirable way.

The dissolution process of oxides in slags has been studied by investigators using rotating rods [5,6] or cylinders [7,8,9] of the dissolving oxide in slag baths. Bygden et al. [5] and Ping and Seetharaman [6] studied the dissolution of MgO in CaO-FeO-SiO_2 and CaO-FeO-CaF_2-SiO_2 respectively and found that the rate limiting step was solid state diffusion through a reaction product layer. X. Yu et al. [7] studied the dissolution of Al_2O_3 in mold slags and concluded that liquid diffusion in the slag was controlling the rate. Taira et al. [9] used a similar approach for Al_2O_3 dissolution in CaO-Al_2O_3-SiO_2 and found that boundary layer diffusion was rate controlling. These reported works were mainly concerned with refractory erosion and thus, the applicability of these results to the kinetics of inclusion dissolution is limited due to the large volume ratio between slag and inclusion in the latter case.

The current work investigates the dissolution kinetics of Al_2O_3 *in situ* in transparent synthetic slags using a confocal scanning laser microscope (CSLM). The objectives of the overall project is to:

- investigate the mechanisms behind inclusion separation across slag metal interfaces and inclusion dissolution in slags
- based on this insight investigate whether slag chemistry can be optimized with respect to inclusion dissolution

2. Materials and methods

A Confocal Scanning Laser Microscope equipped with a gold image furnace was used for studying both separation of inclusions across slag/metal interfaces and dissolution in slags. The principal features and advantages of the 1LM21H™ microscope and hot stage for studying metallurgical melts have been described in literature [10,11]. The principle advantages of this system are that (i) unfocused light is deflected by a pin-hole and (ii) the radiation from the focal plane is detected, a high signal to noise ratio is maintained due to the high intensity of the laser light source.

The inclusion separation studies were performed by placing a 3-4 mm disk of low C-steel killed with Si, Mn and Al on the bottom of a alumina crucible. The rest of the crucible was filled with the slag. Upon heating the slag became transparent after melting and the interface of the molten steel/slag could be observed through the transparent slag. Solid and liquid inclusions at this interface were then observed.

Dissolution studies were performed in a Platinum crucible by placing the inclusions on the surface of a solid slag and heat up this assembly to the desired temperature. Once the slag melted and the inclusion submerged into it, the size of the inclusion was monitored.

Fused Al_2O_3 particles of 50 - 90 μm radius were obtained from Alfa Aesar. To ensure that the bulk composition of the slag remained relatively constant, the amounts of alumina addition were kept below 0.1wt% of the slag samples.

In the case of inclusion separation across slag/metal interfaces, a 50 wt.% CaO-50 wt.%Al_2O_3 slag was used and in the case of dissolution the slag composition was 48 wt. % CaO-48 wt. %Al_2O_3-1.5 wt. % SiO_2 slag,

The experiments were conducted under an ultra high purity Ar atmosphere (Po_2= 10^{-6} atm). The experimental temperature ranges varied depending on the thermodynamics and kinetics of the processes for the various slag systems. The upper limit was defined when the dissolution kinetics was too fast to be measured and the lower temperature limit was when the Al_2O_3 particle no longer dissolved but instead grew by acting as an inoculant for heterogeneous precipitation of solid phases from the liquid slag.

The apparent area of the particles was measured with a public domain image analysis software and the radius of an equivalent circle was computed [12] at defined time intervals. Errors originating from the shadow of the particles on the crucible bottom and the roughness of the particle surface were estimated to contribute a 5 μm error in the equivalent particle radius.

3. Results and discussions

The most dominantly occurring inclusions were alumina rich solid ones and liquid inclusions consisting of 15% Al_2O_3, 11%SiO_2 and 7% MnO. The compositions were measured by analyzing the solid samples through SEM-EDS.

3.1. Separation across slag/metal interfaces

Solid alumina inclusions were observed to rest at the slag metal interface on the slag side. An example is shown in Figure 2. The separation process of this inclusions could not be observed suggesting that they separate during heating or at the beginning of the experiment at a rate that is not observable. What was noticed however was the agglomeration of these inclusions at the slag metal interface, an example of this is shown in Figure 2a-c. This process was not due to the fluid flow in the molten steel or slag since the motion of the moving inclusion could be seen to counter the bulk fluid flow.

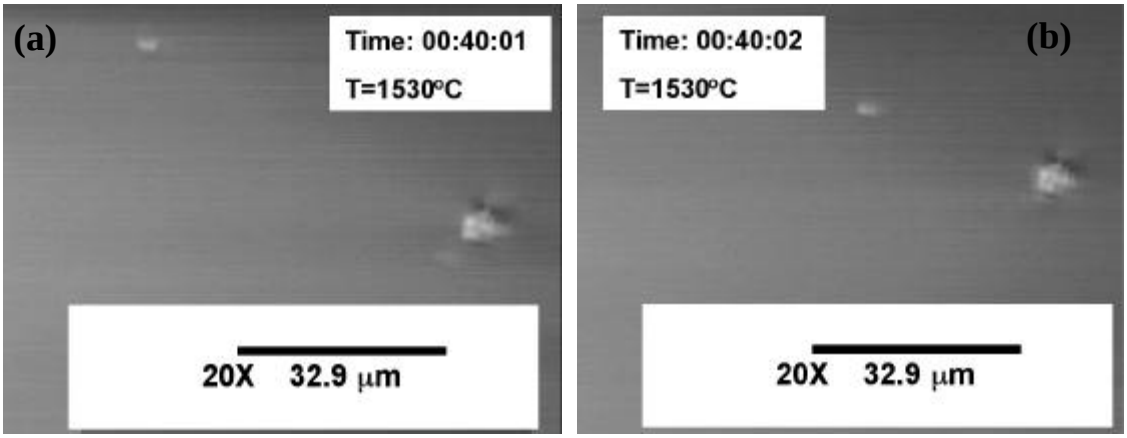

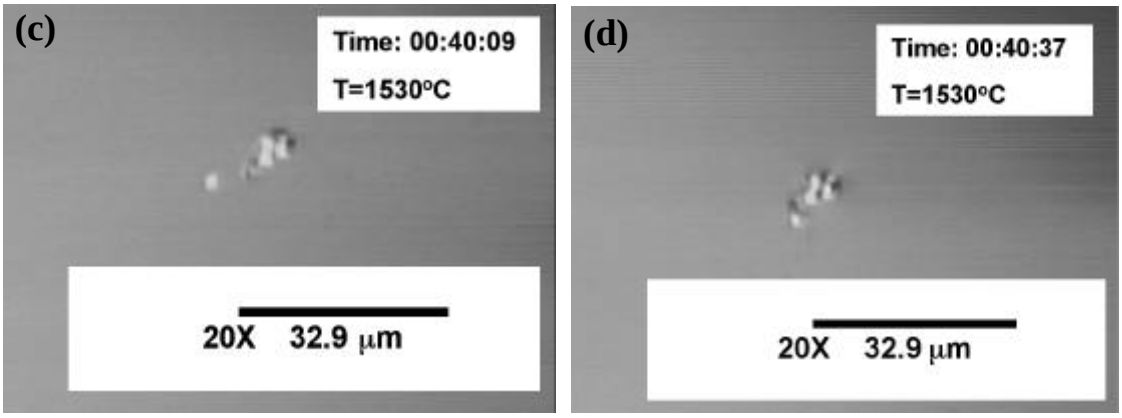

Figure 2a-d. Agglomeration of alumina inclusions at the slag/metal interface

The liquid $MnO\text{-}SiO_2\text{-}Al_2O_3$ inclusions could be seen to separate across the molten steel meniscus. They would start appearing at a certain point at the interface and it took between 2-7 seconds until they emerged on the slag side. They would subsequently disappear (presumable by dissolving into the slag) and create a wake that pushed all adjacent objects away.

3.2. Dissolution of Al_2O_3 in $Al_2O_3/CaO/SiO_2$ slags

The alumina particles started dissolving as soon as they got submerged into the molten slag. An example of the dissolution is shown in Figure 3. The particle never sinks to the bottom but remains suspended in the liquid slag during the dissolution process. Both the particle as well as the slag are semi-transparent in this system and therefore the particle is only easily distinguishable from the slag at its edges.

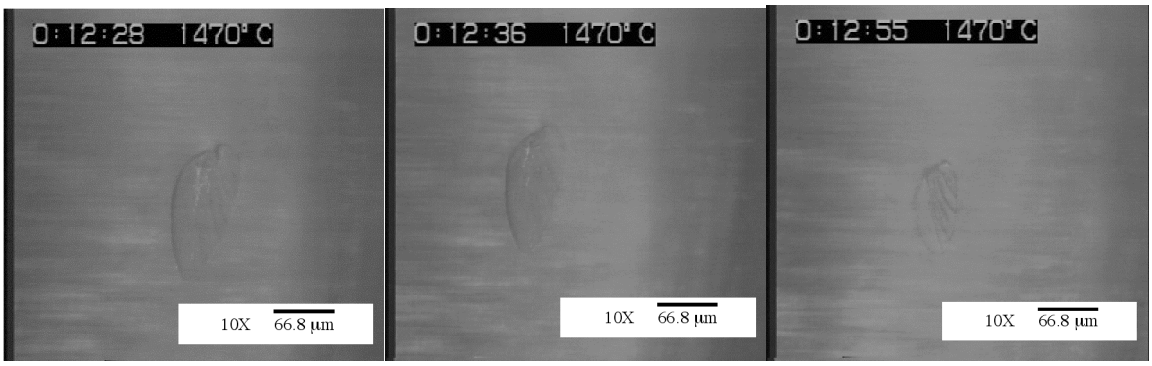

Figure 3. Successive dissolution of an alumina particle inside a semi-transparent slag.

Assuming a topochemical dissolution process, the equivalent circular radius of the inclusion particle was evaluated, using image analysis. The change in this radius with time is shown in Figure 4. Simulated curves according to a boundary layer diffusion controlled mechanism [13] is also plotted in this Figure. The simulated curves were

calculated by estimating the total dissolution time and initial particle radius from the experiments.

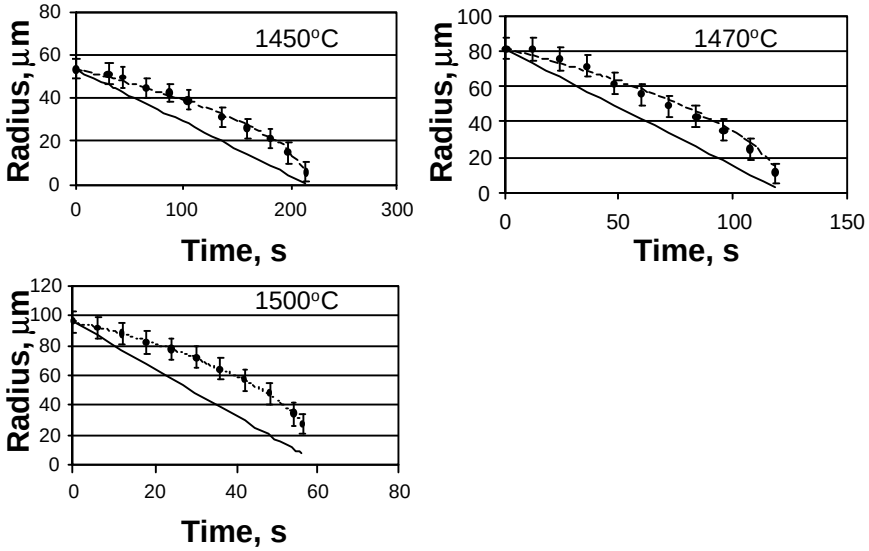

Figure 4. The change in equivalent radius. Solid lines are simulations according to boundary layer diffusion controlled dissolution.

In the case of boundary layer diffusion in the slag phase, the following relations apply [13]:

$$\frac{r_p}{R} = \left(1 - \frac{t}{t}\right)^{1/2} \tag{1}$$

$$t = \frac{r R^2}{2D\left(C^{(p)}_{Al_2O_3} - C^{(slag)}_{Al_2O_3}\right)} \tag{2}$$

Here, r_p and R are the actual and initial radius respectively of the particle, r is the density of the dissolving particle, t and t are the actual and total dissolution times respectively. D is the diffusion constant of the slowest diffusing species resulting from the dissolution process that needs to be transported into the bulk slag across a boundary layer. The value of D is usually expressed as a function of temperature, $D = D_0 \exp(-Q/RT)$. $C^{(p)}_{Al_2O_3} - C^{(slag)}_{Al_2O_3}$ is the concentration difference between the particle and slag. It has been assumed in Equations (1-2) that the fluid flow is within the Stokes law regime where the mass transfer coefficient, k_g is approximated as: $k_g = D/R$.

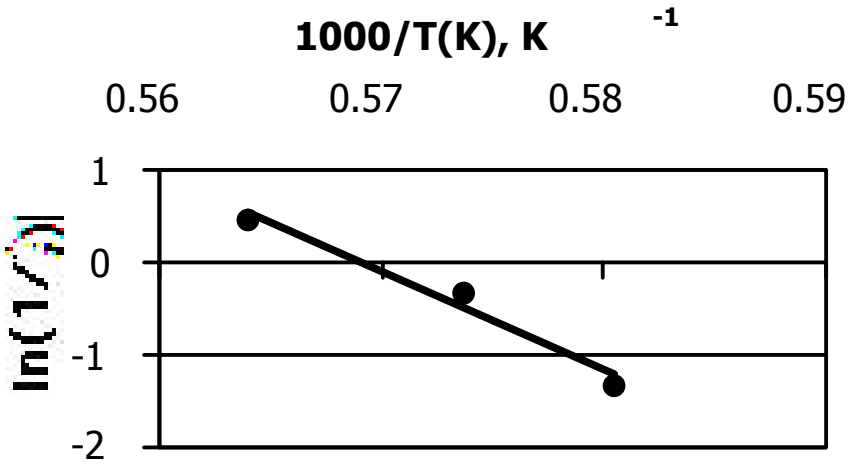

Figure 5. Temperature dependence of the reaction rate

If we assume that density and concentration differences are not dependent on the temperature then the diffusion constant becomes proportional to the inverse of t, $D \propto 1/t$. Therefore we can evaluate the activation energy of diffusion, Q, from the plots of $\log t$ versus 1/T. The calculated activation energy from figure 5 is 1,167kJ.

This activation energy is far larger than the generally reported values of 100~300 kJ [14] for activation energies in this slag system. The large activation energy means that the dissolution is highly accelerated by increasing temperature. One reasons for this is that there is a dependence of the concentration difference upon the temperature. The concentrations of the components of the slag at the slag/particle interface may be the equilibrium concentrations. Thus the concentrations at the interface vary following liquidus line of the phase diagram. Therefore we need measure precise concentrations of liquidus line in order to account for the temperature dependancy of the concentration difference in Equation (2) and thus analyze the dissolution behavior of the solid particles in the slag.

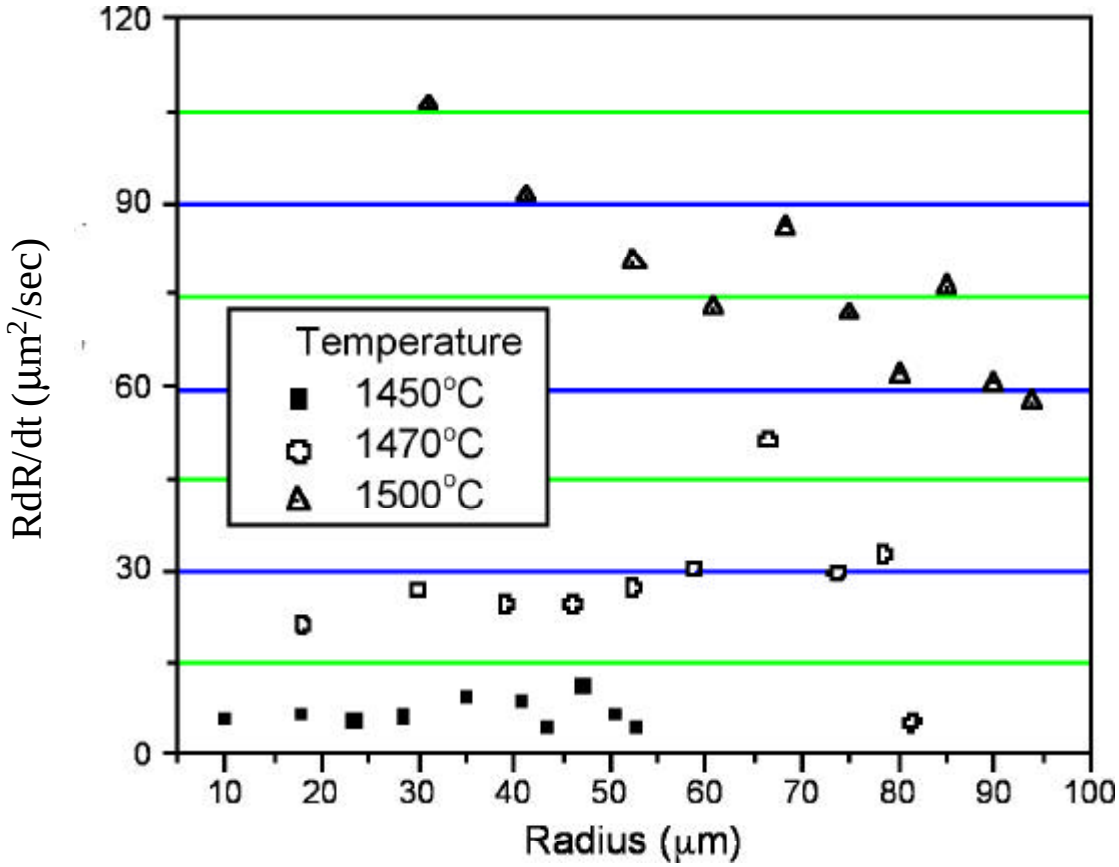

Figure 6. The dissolution velocities at different temperatures.

Another reason for the physically unrealistic activation energy is that the boundary layer thickness or dissolving mechanism changes with temperature. The above described boundary layer diffusion model assumes that the boundary layer thickness is 1/R. Therefore the dissolving velocity ($\frac{dR}{dt}$) of the particle depends on 1/R. Figure 6 shows change of the value of $R \times \frac{dR}{dt}$ versus R. The value of $R \times \frac{dR}{dt}$ is increasing as diameter of the particle is decreasing at 1500 ^{o}C, while it is rather constant at the lower temperatures. This result suggests that at high temperature the dissolving mechanism or at least the behavior of the boundary layer can be changed. To clarify this behavior, the occurrence and effect of fluid flow needs to be studied.

4. **Summary**

- Alumina inclusions separate rapidly across 50% wt. CaO-50%wt. Al_2O_3 slag/metal interfaces but agglomerate with one another once they have separated at the slag side of the interface.
- Observation of dissolution behavior of alumina particles in the slag system: 48 wt. % CaO-48 wt. %Al_2O_3-1.5 wt. % SiO_2 was investigated and the results suggest that a

boundary layer controlling model can be used to explain the dissolution behavior. The calculated apparent activation energy is however far to large to be explained by diffusion and the effect of the change with temperature of the concentration difference between the particle/slag interface and bulk slag needs to be incorporated.

- At 1500^{o}C an analysis based on a boundary layer model suggests that the boundary layer thickness changes with time and hence the effect of fluid flow needs to be considered.

5. **Acknowledgements**

The authors would like to thank the member companies of the Center of Iron and Steel Research for their support.

5. References

1. A.W. Cramb: Impurities in Engineering Materials, Edited by C.L. Briant, Chapter 4, 1999, Marcel Dekker, Inc. ISBN 0-8247-9965-8, pp. 49-90

2. K. Marukawa and H. Kasima: The Refining Limit of Impurity Elements in Mass Production, ISIJ, Tokyo, 1996, pp. 1-4

3 . C.F. Orrling, S.Sridhar and A.W. Cramb: In prep. To be submitted for the 6th International Conference on Molten Slags, Fluxes and Salts, 2000, Stockholm

4 . K.C. Mills et al.: *Ironmaking and Steelmaking*, 1991, vol. 18, pp. 258-265

5. J. Bygden, T. DebRoy and S. Seetharaman: *Ironmaking and Steelmaking*, 1994, vol. 21 (4), pp. 318-323

6. P. Zhang and S. Seetharaman: *J. Am. Ceram. Soc*., 1994, vol. 77 (4), pp. 970-976

7. X. Yu, R.J. Pomfret and K.S. Coley: *Met. And Mat. Trans.*, 1997, vol. 28B, pp. 275-279

8. A.R. Cooper Jr. and W.D.K.J. Kingerey: J. Amer. Ceram. Soc., 1964, vol. 47 (1), pp. 37-43

9. S. Taira, K, Nakashima and K. Mori: *ISIJ International*, vol. 33 (1), 1993, pp.116-123

10 H. Chikama et al., Materials Transactions, *JIM*, vol. 37 (4), 1996, pp. 620–626.

11 . C. Orrling, Y. Fang, N. Phinichka, S. Sridhar, and A.W. Cramb: *JOM-e*, 1999, vol. 51, (7), http://www.tms.org/pubs/journals/JOM/9907/Orrling/Orrling-9907.html

12. NIH Image, version 1.62, developed at U.S. National Institutes of Health and available on the Internet at http://rsb.info.nih.gov/nih-image/

13 O. Levenspiel: Chemical Reaction Engineering, Chapter 25, 3rd Edition, 1999, John Wiley & Sons, ISBN 0-471-25424-X, pp. 566-586

14 K.C. Mills: SLAG ATLAS (2nd Edition) Edited by Verein Deutscher Eisenhüttenleute, 1995, Verlag Stahleisen GmbH, Düsseldorf, p. 547